HEAT TRANSFER THROUGH POROUS MEDIA IN STATIC SUPERFLUID HELIUM

B. Baudouy[1], F.-P. Juster[1], H. Allain[1], E. Prouzet[2], A. Larbot[2] and R. Maekawa[3]

[1] CEA/Saclay, DSM/DAPNIA/SACM
91191 Gif-sur-Yvette CEDEX, France

[2] Institut Européen des Membranes, CNRS, ENSCM, UM II
34293 Montpellier CEDEX 5, France

[3] National Institute of Fusion Science, Cryogenic Laboratory
Oroshi-cho, Toki, GIFU, 509-5292, Japan

KEYWORDS: heat transfer, porous media, helium 4 superfluid phase
PACS: 44.30.+v, 67.40.-w

ABSTRACT

Heat transfer through porous media in static saturated superfluid helium is investigated for porous media with different thickness, porosity and pore size. For large pore diameter, data are analyzed with the tortuosity concept in the pure Gorter-Mellink regime. It is shown that the tortuosity is constant over the temperature range investigated. For smaller pore diameter, the analysis reveals that the permeability is temperature-dependent in the Landau regime. In the intermediate regime, a model, including Landau and Gorter-Mellink regime, predicts a constant tortuosity within 10% but falls short predicting correctly the experimental data over the entire range of temperature.

INTRODUCTION

For the next generation of particles accelerator high field magnets, the use of Nb_3Sn superconductor is considered. Higher heat deposition than in current accelerator magnets is expected and new electrical insulation is under development for improved cooling efficiency. Ceramic materials based insulation are investigated as a possible candidate for this purpose [1]. Such insulation with good wrapping capability and excellent resistance to heat would reduce coil fabrication complexity and costs. These materials, however, can possess porosity much lower than conventional electrical insulation and this would reduce cooling efficiency. Since the accelerator magnet electrical insulation constitutes the main thermal resistance to He II cooling [2, 3], heat transfer studies on porous media are carried out with the focus on large heat flux and large temperature differences [4].

EXPERIMENTAL SET-UP AND SAMPLE

Two types of porous media, which differ in geometrical properties, are tested in this study (see TABLE 1). The CSi samples, made at Institut Européen des Membranes, have much larger average pore diameter and are suited for the study in the pure Gorter-Mellink regime. The 97 % pure Al_2O_3 samples are commercial porous cylindrical plate and are suited for the study in the intermediate regime (Landau + Gorter-Mellink). Each sample is glued in a "sandwich" manner between two G10 circular plates with a hole in the middle to create the heat transfer cross-sectional area. The "sandwich" is then glued to a stainless steel support flange as FIGURE 1 illustrates.

The experimental set-up was modified from the previous version to eliminate the double vacuum cans and indium joints, which made leak tight experiments difficult [4]. The set-up consists of a stainless steel cylindrical vacuum can, creating a thermal insulation between the heated inner bath and the He II bath (FIGURE 1). The instrumentation is composed of a silicon piezo-resistive pressure sensor, two Allen Bradley carbon resistors, one located in the inner bath (T_i) and the other in the cryostat bath (T_b), and a heater located in the inner bath. The temperature measurement sensitivity is within the range of ± 20 μK to ± 200 μK between 1.4 K and 2.0 K. The temperature difference error is at most ±0.2 mK in the range of our investigation. Total heat flux is generated with a 0.5% uncertainty. The He II bath temperature is regulated to within 1 mK, during an hour, via the regulation of the pressure above the liquid surface. More details on the experimental set-up, procedure and instrumentation can be found in [4].

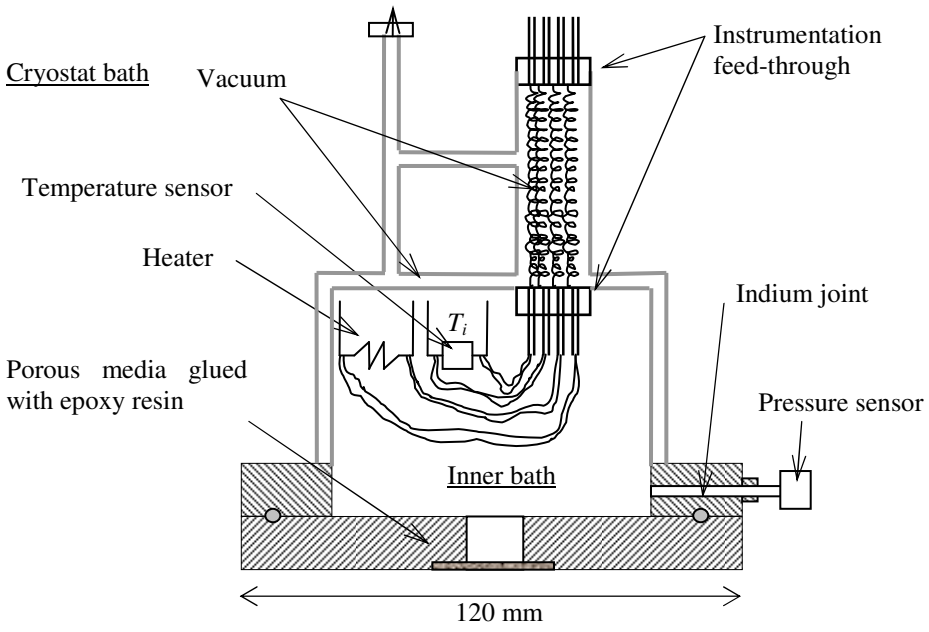

FIGURE 1. Schematic of the experimental set-up.

TABLE 1. Properties of the Porous Media

Material	Al_2O_3	CSi#1	CSi#2
Average Pore Diameter (μm)	2	20	10.8
Porosity, ε (%)	32	58	62
Thickness, e (mm)	2, 3 and 4	1.2	1.5
Cross-Sectional Area, A ($\times 10^6$ m^2)	2 mm : 300 3 mm : 402 4 mm : 305	20.7	16.0

TORTUOSITY CONCEPT

In porous media geometry, the average length of the flux line (heat or flow) going through the sample is longer than the thickness as FIGURE 2 demonstrates. The ratio of the average length of the flux line to the thickness of the sample is called the tortuosity [5]. In a one dimensional media, the tortuosity is reduced to a scalar value, ω. A gradient, such as the temperature gradient for example, is written as

$$\vec{\nabla}T = \frac{dT}{dx} \approx \frac{\Delta T}{\ell} = \frac{1}{\omega}\vec{\nabla}T_e, \tag{1}$$

where $\vec{\nabla}T$ and $\vec{\nabla}T_e$ are respectively the temperature gradient with respect to the length of the flux line and the thickness of the sample. Note that the concept of tortuosity has a meaning only when the heat travels in the fluid phase, *i.e.* there is no heat transfer coupling between the liquid and the solid (porous medium). If we consider that there is n identical unit channels with the same cross-sectional area of A_{uc} and same length of $e\omega$. The volume of the n channels is $nA_{uc}e\omega$. As the total sample volume is Ae and the volume of the n channels (void) is εAe, we can deduce that the cross-sectional area of the n channels is $nA_{uc}=\varepsilon A/\omega$, which implies that the heat flux density with respect to the flux line is,

$$q = \omega\frac{Q}{\varepsilon A} = \omega q_e. \tag{2}$$

LANDAU REGIME

In the low heat flux regime, the pressure gradient is proportional to the temperature gradient,

$$\vec{\nabla}p = \rho s\vec{\nabla}T \tag{3}$$

where p, ρ, s and T are the pressure, the density, the entropy and the temperature of helium. This equation is known as the London equation and it is derived from the Navier-Stokes equations applied to superfluid helium [6]. For the three Al_2O_3 samples, the FIGURE 3 demonstrates the validity of equation (3) in porous media for low heat flux at different bath temperatures. The solid lines in FIGURE 3 are generated using equation (3) based on the 2 mm sample data. The experimental data agree with the theory for small gradients and the results are independent of the thickness of the sample on the contrary of our first results [4]. The deviation of the data from equation (3) constitutes the evidence of the apparition of vortices and should indicate a critical heat flux. Regrettably as the present study focuses

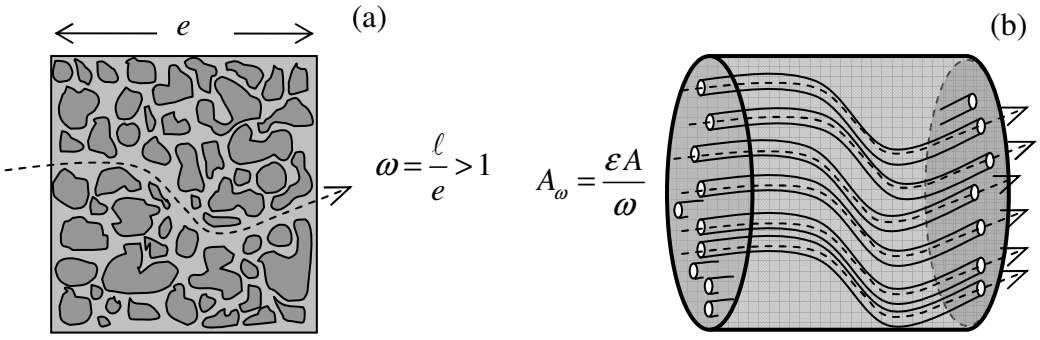

FIGURE 2. Tortuosity principle model for one dimensional media. (a) Definition of the tortuosity for a one dimensional medium. (b) Definition of the effective cross-sectional area.

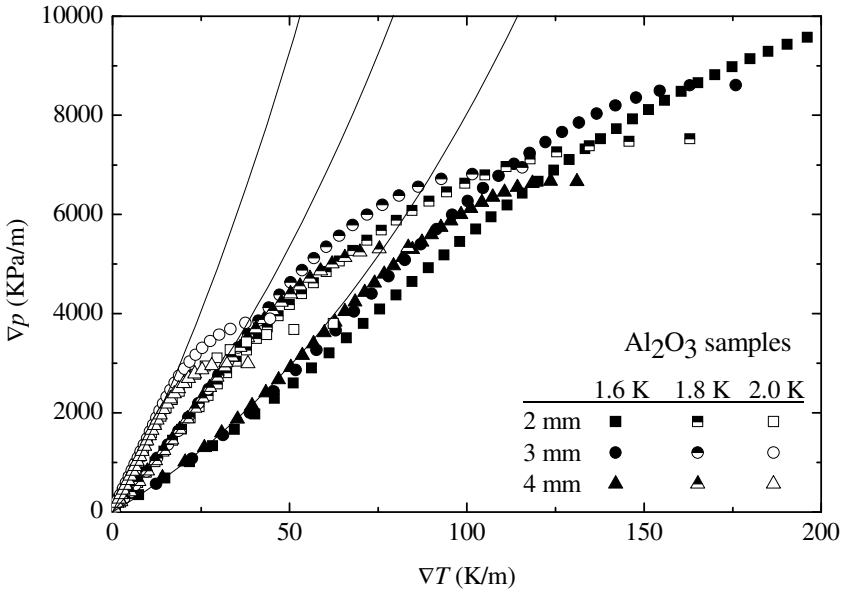

FIGURE 3. Evolution of ∇p with ∇T and the comparison with equation (3).

on large heat flux and large temperature difference, few data points were taken in the low q-ΔT range as the FIGURE 4 depicts. It is therefore difficult to extract accurately the information on critical heat flux.

The pressure gradient causes a laminar flow and the Darcy law was found to be valid in porous media using the velocity of the normal fluid v_n (see [7] for example). When the tortuosity is introduced, the pressure gradient becomes,

$$\vec{\nabla} p_e = \omega \mu_n \frac{\vec{v}_n}{K_e}, \tag{4}$$

where μ_n is the viscosity of the normal fluid component and K_e the permeability of the porous medium. The heat flux q is related to v_n by $q=\rho s T v_n$ in zero net mass flow (ZNMF) where the bulk mass flow is null ($\rho_n|v_n|+ \rho_s|v_s|=0$). Equation (4) is transformed then in terms of a q_e-∇T_e relation using equation (3) and is integrated because the variation of the physical properties with the temperature needs to be taken in account,

$$q_e = K \frac{1}{e} \int \frac{(\rho s)^2 T}{\mu_n} dT, \tag{5}$$

where we use an averaged permeability $K=K_e/\omega^2$. The reason to include the tortuosity ω in the permeability is motivated by the fact that it is not clear that the Darcy law is intrinsically a function of the thickness of the sample or the average length of the flux line. Furthermore, it will not be an unpardonable mistake since the heat transfer in porous media in the Landau regime depends on both parameters, assuming that ω is only dependent on geometry. In addition, a couple of remarks can be made on the validity of equation (5) to analyze heat transfer data in porous media. First, equation (5) is based on the assumption that the Darcy law is valid in heat transfer experiments, which is questionable since it was developed for isothermal flow. Moreover, it is evident that the permeability is temperature dependent as is the viscosity (equation (4)) [8]. Some groups are even looking at the modification of the Darcy law due to the effect of non isothermal flow [9]. The second remark is that the permeability deduced from equation (5) is an average value over the range of temperature assuming that the Darcy law is not modified for the investigated range of temperature. This assumption should also be verified. Having these arguments in

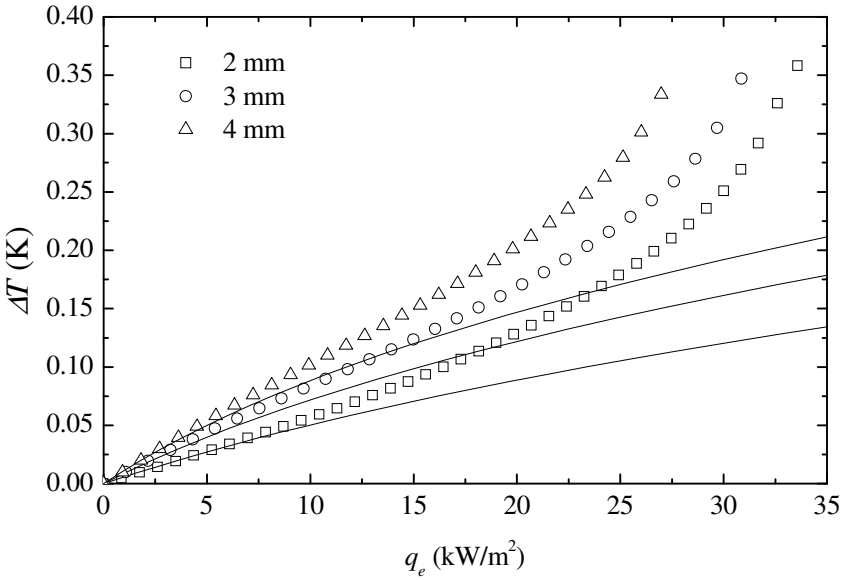

FIGURE 4. Evolution of ΔT with q_e at 1.8 K and comparison with equation (5) for the Al_2O_3 samples.

mind, it is not surprising that a temperature dependent permeability is found in our study. Equation (5), displayed as solid lines in FIGURE 4 with results at 1.8 K, lead to a permeability between 3.6 and 3.8 10^{-14} m^2 as FIGURE 5 depicts it. It needs to be noted that the cross-sectional area used to calculate q_e for the 2 mm sample was reduced intentionally from 4.5 (measured) to 3.0×10^{-4} m^2 to match the ∇p-q_e and ∇T-q_e results of other samples. We have no explanation to this other than evoking a partial plug in the sample. Noting that the results displayed in FIGURE 3 agree with the theory, we are confident that this modification reflects the true phenomenon. FIGURE 5 presents the evolution of the permeability with temperature and an average value $\overline{K}$ constructed with results from the three samples. Most of the K values found for the three samples are within a dispersion of 10%. It appears that K decreases with temperature up to 1.8 K and increases above, reflecting the temperature dependency of the viscosity of He II between 1.4 K and 2.1 K. Refined measurements are needed to confirm the temperature dependency of K.

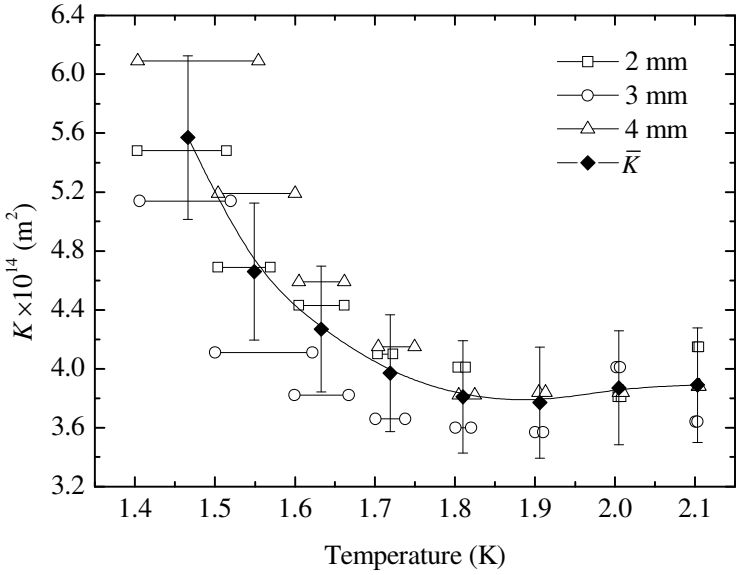

FIGURE 5. Permeability as a function of temperature. Hollow symbols represent the result of the fitting with equation (5). Note the large temperature range used for the fit at lower temperatures. $\overline{K}$ is the average value of K for the three samples. A 10% deviation of the $\overline{K}$ value is plotted to compare with the data dispersion.

PURE GORTER-MELLINK REGIME

In the Gorter-Mellink regime, the relationship between the temperature gradient and the heat flux is given by

$$\left|\vec{\nabla}T\right| = \frac{A\rho_n}{s^4(\rho_s T)^3} q^3, \tag{6}$$

which is transformed, when expressed with respect to the thickness of the sample, into

$$q_e{}^3 e = \frac{1}{\omega^4} \int \frac{s^4(\rho_s T)^3}{A\rho_n} dT, \tag{7}$$

where A, ρ_n, ρ_n and s are the Gorter-Mellink coefficient, the normal and superfluid component density and the entropy. FIGURE 6 shows the steady-state temperature gradient and the heat flux of the sample CSi#1 for different bath temperatures. For each bath temperature the tortuosity ω was extracted from the best fit. On average the relative error between the estimated heat flux and the experimental one is around 10% for the range of temperature investigated. The relative error is higher for lower bath temperature (around 12% at 1.4 K) and reduces as the bath temperature increases (around 7% at 2.1 K). The results for the two CSi samples are presented in TABLE 2. The tortuosity is found to be constant within 10% for both samples showing that the tortuosity concept is valid to a first approximation in ZNMF. Nevertheless one can see in FIGURE 6 that equation (7) under estimates the ∇T_e at low heat flux and over estimates them for high heat flux. For any bath temperature, the estimated ∇T_e can be two times smaller than the experimental value at low heat flux whereas at higher heat flux it is lower by 10% only. One can also note that ω is found to be lower at 2.1 K for both samples and could be attributed to the accuracy of the physical properties of He II close to T_λ.

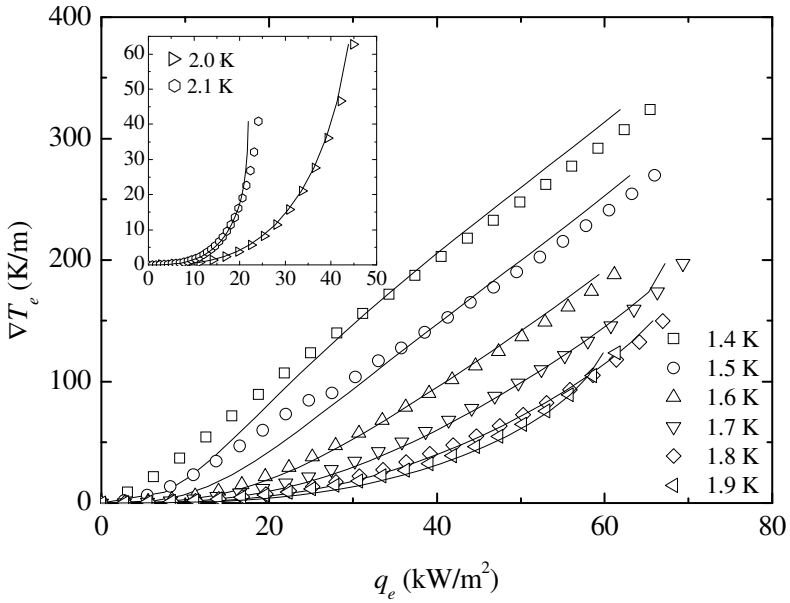

FIGURE 6. Temperature gradient as a function of the heat flux for different bath temperature for the sample CSi #1. The experimental results are shown with hollow symbols and equation (7) is displayed as solid line.

TABLE 2. Tortuosity, ω

Bath temperature (K)	1.4	1.5	1.6	1.7	1.8	1.9	2.0	2.1
CSi#1	1.71	1.74	1.75	1.77	1.79	1.81	1.78	1.67
CSi#2	1.58	1.61	1.61	1.63	1.65	1.65	1.61	1.49

INTERMEDIATE REGIME

In this regime it is assumed that another dissipative force due to interactions between the two components of the liquid exists. Assuming that the transition from laminar to turbulent flow is smooth, the temperature gradient is expressed for a porous medium in ZNMF by rearranging the Navier-Stokes equations as,

$$\left|\vec{\nabla}T_e\right| = \frac{1}{K}\frac{\mu_n}{(\rho s)^2 T} q_e + \omega^4 \frac{A\rho_n}{s^4(\rho_s T)^3} q_e^{\,3}. \tag{8}$$

The use of equation (8) assumes that the flow of the normal component is laminar and that the term $\rho_n.\nabla v_n$ is neglected in the particular derivative of the momentum conservation equation of the normal fluid.

To analyze the data, equation (8) has been numerically integrated over a ΔT range to take into account the temperature dependency of the physical properties. The analysis consists of minimizing the average value of the relative error $|(q_e\text{-}q_{Eq.(8)})/q_{Eq.(8)}|$ over the entire range of ΔT by adjusting the tortuosity ω, where q_e and $q_{Eq.(8)}$ are respectively the experimental heat flux and the one given by equation (8). The permeability used in the model is identical for all three samples and $\overline{K}$ is presented in FIGURE 5. The evolution of ∇T_e with q_e is compared with equation (8) in FIGURE 7 for the three samples at 1.8 K. The average relative error over the entire range of heat flux between equation (8) and the data is between 5 and 10%. But at low heat flux the error can be as high as 50% while at high heat flux it is around 10%, with the model always over estimating the results. This is certainly due to the fact that the Gorter-Mellink term should be null in equation (8) since it is considered that the superfluid turbulence appears after a threshold, *i.e.* critical heat flux.

Although fair agreement between equation (8) and the data was found, the tortuosity extracted with equation (8) is not independent of temperature. FIGURE 8 presents the results of the tortuosity found as a function of temperature for the three samples. The permeability decreases with temperature. On average the sensibility of the tortuosity to the permeability is small since the variation of the tortuosity is less than 5% for a 10% deviation in the permeability. If the tortuosity is only geometry dependent, equation (8)

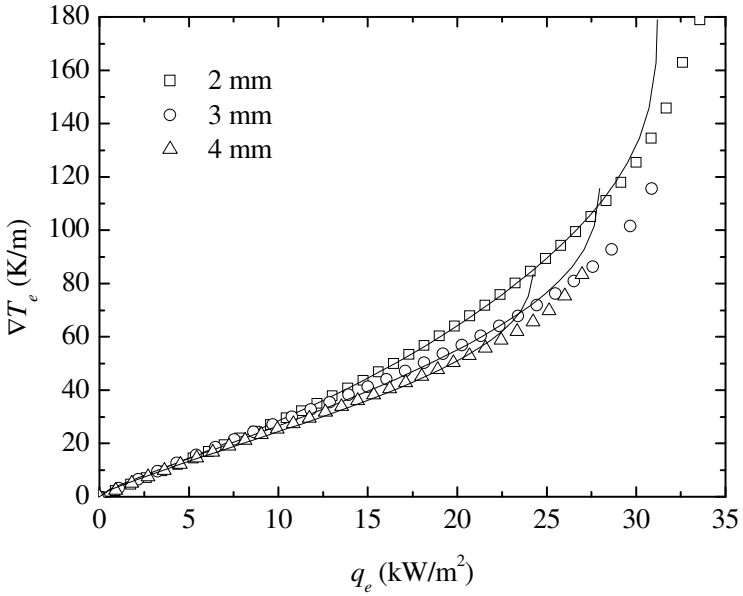

FIGURE 7 . Evolution of ∇T_e with q_e at 1.8 K for the Al_2O_3 samples. The experimental results are shown with hollow symbols and equation (8) is displayed as solid line.

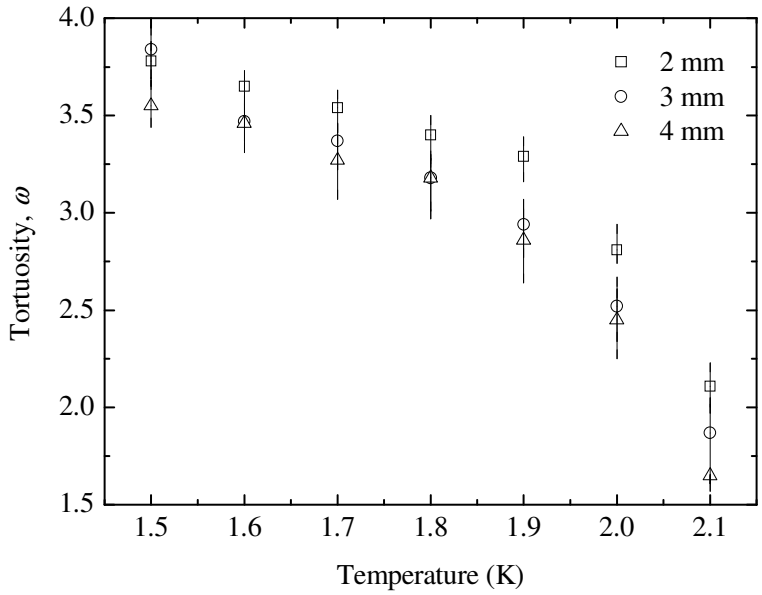

FIGURE 8. ω as a function of temperature. Vertical lines represent the variation of the tortuosity for a 10% variation of the permeability

fails to predict correctly the evolution of tortuosity. But the results found in pure Gorter-Mellink regime suggest that the tortuosity at the highest temperature may be neglected. That is, if we consider the evolution of the tortuosity up to 1.9 K, an average value is nearly independent and is given as ω=3.4±0.4, which corresponds to 10% variation.

CONCLUSION

In a pure Gorter-Mellink regime, data fitted with a 1D tortuosity concept to within 10% in average, constituting the evidence that the tortuosity concept can be applied to He II in porous media. For smaller pore size diameter (1 μm), it is shown that the permeability is temperature dependent in the Landau regime. More work is needed to analyze the temperature dependency and the validity of the Darcy law. In the intermediate regime, a model including Landau and Gorter-Mellink regimes remains insufficient to predict correctly the experimental data over the entire range of temperature but if we consider the evolution of the tortuosity up to 1.9 K, a constant value can be given within 10% variation.

REFERENCES

1. Puigsegur, A.*, et al.*, "Development of an innovative insulation for Nb_3Sn wind and react coils," in *Advances in Cryogenic Engineering (Materials)* 50A, edited by U. Balachandran, AIP, New-York, 2004, pp. 266-272.
2. Meuris, C.*, et al.*, *Cryogenics,* **39**, pp. 921-931, (1999).
3. Baudouy, B.*, et al.*, *Cryogenics,* **40**, pp. 127-136, (2000).
4. Maekawa, R. and Baudouy, B., "Heat transfer through porous media in the counterflow regime of He II," in *Advances in Cryogenic Engineering* 49, edited by J. Waynert, AIP, New York, 2004, pp. 983-990.
5. Kaviany, M., *Principles of convective heat transfer*, Springer-Verlag, New York, 1994.
6. Putterman, S. J., *Superfluid Hydrodynamics*, North-Holland /American Elsevier, 1974.
7. Yuan, S. W. K. and Frederking, T. H. K., "Darcy Law of Thermo-Osmosis for Zero Net Mass Flow at Low Temperatures," in *ASME-JSME Thermal Engineering Conference* 2, edited by 1983, pp. 191-197.
8. Nield, A. D. and Bejan, A., *Convection in porous media*, Springer, 1998.
9. Narasimhan, A. and Lage, J. L., *Journal of Heat Transfer,* **123**, pp. 31-38, (2001).